G. M. Lederle

Heat-transfer Calculations at the Tape-head Interface of a Computer Tape Drive

Abstract: Frictional heat generation can develop localized high temperatures at the tape-head interface of a computer tape drive and can seriously affect the performance of the drive. Using standard heat transfer theory, we calculated the magnitude of this "hot spotting" to be of the order of 21°C for an IBM 2400 series tape drive. In general, it is almost impossible to accurately measure hot spotting on a tape drive. A series of calculations was performed to investigate why this is so.

Introduction

Sliding systems can generate localized high temperatures, or hot spots, at points of true contact between the sliding bodies. When a polymeric tape slides across the metallic head of a computer tape drive, the heat generated can become high enough to intermittently bond the tape to the surface of the head. The continual forming and breaking of such bonds produces wear debris that gives rise to "adhesive wear," a common cause of failure. Also, in a tape-head system that has been run and then allowed to cool with tape and head in static contact, the heat buildup can cause more permanent sticking and may even prevent the tape drive from starting again. For these and other reasons relating directly to tape drive performance, it is important to determine the extent of hot spotting at the tape-head interface.

In the past, attempts have been made to assess the degree of hot spotting, both by calculation and by measurement, but neither approach has yielded satisfactory results. The difficulty with the calculations has been that various theoretical models were based on several questionable assumptions. In addition, a number of operating parameters needed for the calculation are not easily determined. The disadvantages of experimental measurement depend upon the technique used. With one of the more popular methods, the use of infrared sensing devices, it is generally not possible to make an *in situ* measurement. The problem in this instance is to derive the temperature rise at the hot spot from a measured value that is displaced in both time and space from the point of contact between the bodies.

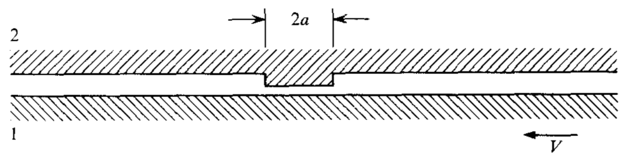

Figure 1 Sliding contact at a square junction.

This paper presents a theoretical analysis of the hot spotting that occurs at the tape-head interface of an IBM 2400 series tape drive. Details are given to justify all major assumptions made in the calculations. The analysis is also used to examine why direct measurement of hot spotting has been unsuccessful.

A model for hot spotting

Jaeger [1] has developed a model for calculating the frictional temperature buildup between two semi-infinite bodies that are in sliding contact over a square contact area, having side $2a$ as indicated in Fig. 1. If all surface heat transfer is restricted to this junction, then at steady state, the average temperature rise T of the junction is given by

$$T = \frac{k_1^{\frac{1}{2}} \mu W g V}{3.76 a J (1.125 K_2 k_1^{\frac{1}{2}} + K_1 \sqrt{a V})}, \qquad (1)$$

where

g = 980 cm/sec^2
J = 4.18 $\times$ 10^7(gm)(cm^2)/(sec^2)(cal), the mechanical equivalent of heat
K is thermal conductivity
k is thermal diffusivity
μ is the dynamic coefficient of friction
V is the relative velocity of the two bodies
W is the load borne by the junction,

and the subscripts 1 and 2 refer to the two sliding bodies designated in Fig. 1.

A description of the individual contact junction

In order to apply Eq. (1) to a given tape-head contact junction, reliable determinations of a, the radius of the contact junction, and W, the load borne by it, are needed. The most direct method of obtaining W would be to determine how the macroscopic load is distributed over the individual contact points between the two bodies, but this approach would be extremely impractical. Instead, it is generally recognized that the real contact area for the system will be a very small fraction of the apparent contact area. Therefore, even a light load on the tape will cause plastic deformation of the polymeric asperities that are in actual contact with the head [2]. For this condition,

$$W = \pi a^2 p_m \tag{2}$$

where p_m, the mean pressure over the area of true contact, is [3]

$$p_m \simeq 3Y. \tag{3}$$

By Eqs. (2) and (3), the load on the individual asperity can be expressed directly in terms of the yield stress of the polymeric tape coating Y and the contact radius of the asperity a. Therefore, Eq. (1) can be rewritten

$$T = \frac{2.5 k_1^{\frac{1}{2}} \mu Y g V a / J}{1.125 K_2 k_1^{\frac{1}{2}} + K_1 \sqrt{a V}}. \tag{4}$$

Rabinowicz [4] has formulated an indirect method of calculating a which he has used to produce reliable estimates of the contact radius for a wide variety of sliding surfaces. It is based on the hypotheses that a wear particle and the contact area at which it is formed are equal in size, and that a wear particle is produced when the stored elastic energy of the particle exceeds the increase in surface energy that occurs during its formation. His equation

$$a = 4000\gamma/Y \tag{5}$$

introduces an additional material property γ, the surface tension of the tape coating.

Material and operating constants

The physical constants and operating variables for an IBM 2400 series tape drive and for IBM Series/500 magnetic tape have been chosen to illustrate the hot-spotting calculation. For these systems, the tape velocity and dynamic coefficient of friction over the tape drive head are [5]

$$V = 285 \text{ cm/sec} \quad \text{and} \tag{6}$$

$$\mu = 0.442. \tag{7}$$

The required thermal and physical properties of the tape coating (polymer and γ-Fe_2O_3 particles) are

$$k = 7.9 \times 10^{-4} \text{ cm}^2/\text{sec} \tag{8}$$

$$K = 4.25 \times 10^{-4} \text{ cal/(sec)(°C)(cm)} \tag{9}$$

$$Y = 2.6 \times 10^8 \text{ dynes/cm}^2 \tag{10}$$

$$\gamma = 38 \text{ dynes/cm} \tag{11}$$

and, for the HyMu "80"* epoxy head,

$$k = 0.06 \text{ cm}^2/\text{sec} \tag{12}$$

$$K = 0.06 \text{ cal/(sec)(°C)(cm)}. \tag{13}$$

The yield stress Y of the tape coating was measured [6] at a testing rate of 0.25 in/in/min and then converted to a value at 7 $\times$ 10^4 in/in/min, the rate of deformation at the tape-head interface, by means of a WLF time-temperature superposition [7]. According to Rabinowicz's Eq. (5) and expressions (10) and (11), the contact radius is

$$a = 5.9 \times 10^{-4} \text{ cm}. \tag{14}$$

The calculation of hot spotting

Once estimates for all the necessary parameters have been developed, we can calculate the temperature rise at the contact junctions of the tape-head interface. If the sliding contact is considered to be carried by the tape (phase 2 in Fig. 1), then according to Eqs. (4), (6), (7), (9), (10), (12), (13) and (14),

$$T = 11.5\text{°C}. \tag{15}$$

If instead the sliding contact is taken to be carried by the head, then according to Eqs. (4), (6–10), (13) and (14),

$$T = 15.6\text{°C}. \tag{16}$$

Considering the nature of the assumptions made in these calculations, the values in Eqs. (15) and (16) do not differ significantly. For purposes of illustration, Eq. (15) is used to represent the actual temperature rise in the calculations that follow.

The accuracy of the result given by expression (15) will depend, in some measure, on the correctness of the

*Trademark Registered, Carpenter Steel Co.

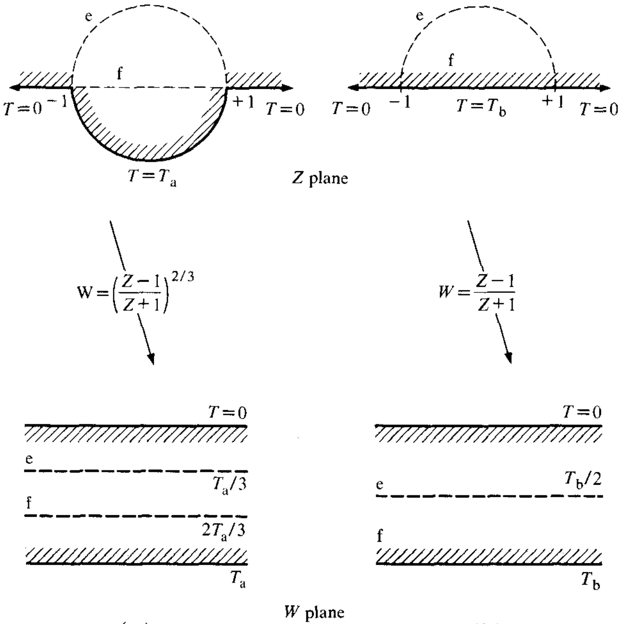

Figure 2 Conformal mapping of asperities into simple geometries. (a) For a raised asperity; (b) for a flat asperity.

Figure 3 Shape of an average tape asperity.

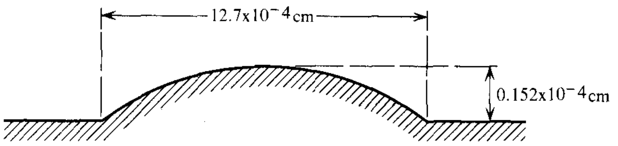

assumptions made in applying Eq. (4) to a tape-head contact junction. Several of these assumptions will now be examined in detail.

- *The assumption of a flat asperity*

In applying Eq. (1) to a tape-head contact junction, we implicitly assumed that the contact area of the sliding junction lay entirely within the plane of the sliding surface. In practice, however, the average contacting asperity protrudes somewhat above the surface of the body and, because of the heat-concentrating effect of such a geometry, can be expected to generate higher surface temperatures than we predicted from Eq. (1).

To estimate the difference involved, we used the two-dimensional system pictured in Fig. 2. Part (a) represents a raised asperity and part (b) an asperity in the plane of the surface. In each case, we maintain a constant rate of heat input across the surface between points -1 and $+1$, and keep all the surface adjacent to this heat source at 0°C. The question is, given the same rate of heat input to both bodies, would the temperature T_a of the raised asperity be significantly higher than the temperature T_b of the flat asperity at steady state?

Conformal mappings that transform both bodies into semi-infinite slabs for which the temperature gradients are known to be linear functions of position are shown in Fig. 2. Note that the temperature gradient between surfaces e and f in Fig. 2(a) is proportional to $T_a/3$, whereas that between the same two surfaces in Fig. 2(b) is proportional to $T_b/2$. Since the heat flow through these two semicircular regions is equal, and if their thermal conductivities are considered equal, it follows that

$$T_a/3 = T_b/2 \tag{17}$$

or

$$T_a = 1.5T_b. \tag{18}$$

Equation (18) indicates that the assumption of a flat contact area will result in a calculated temperature rise which is only $\frac{1}{3}$ lower than the true value. Furthermore, this difference may be even smaller since our surface profile measurements of tape-surface roughness show that the average asperity (Fig. 3) is actually much flatter than that shown in Fig. 2(a). Hence it appears that the assumption of a completely flat asperity does not introduce any serious error into the calculations.

- *The assumption of semi-infinite bodies*

The temperature beneath a circular heat source of radius a on the surface of a semi-infinite body is given [8] by

$$T(z,\, t) = \frac{2q(kt)^{\frac{1}{2}}}{K}\left[\operatorname{ierfc}\frac{z}{2(kt)^{\frac{1}{2}}} - \operatorname{ierfc}\frac{(z^2+a^2)^{\frac{1}{2}}}{2(kt)^{\frac{1}{2}}}\right], \tag{19}$$

where

a is the circular heat source radius
z is the distance below the center of the source
t is time
q is the heat flux per unit area
ierfc is the integral of the complementary error function.

At steady state, Eq. (19) reduces to

$$\frac{T(z)}{T(0)} = -\frac{z}{a} + \left[1 + \left(\frac{z}{a}\right)^2\right]^{\frac{1}{2}}, \tag{20}$$

where $T(z)$ has been normalized by the surface temperature $T(0)$. We can now use this equation to estimate the thermal penetration into the tape and head near a contact junction.

IBM Series/500 magnetic tape is 4.82×10^{-3} cm thick [5], which is equivalent to 8.2 contact radii according to expression (14). Equation (20) predicts that for equilibrium conditions, the temperature will have decreased to 6% of its surface value at a depth of 8.2 contact radii. The percentage would be even less for the more realistic case of a moving heat source, and it is therefore reasonable to assume that for purposes of heat transfer, the tape behaves as if it were infinitely thick. The head is many times thicker than the tape; hence it can also be treated as being infinitely thick with respect to heat transfer.

- *The assumption of noninteracting hot spots*

Before discussing this assumption, we must estimate the spacing and orientation of hot spots at the tape-head interface. The dynamic tensile loading of the tape in an IBM 2400 series tape drive is indicated in Fig. 4. It follows that the normal load borne by the contact area is

$$L \simeq 2(160) \sin 7° = 39 \text{ gm}. \quad (21)$$

Since the points of actual contact can be expected to be plastically deformed [2, 9], the total area of real contact can be calculated from expressions (10) and (21):

$$A_r = L/Y = 1.47 \times 10^{-4} \text{ cm}^2. \quad (22)$$

The total area of *apparent* contact was estimated from the wear scar on a typically worn head to be

$$A_a = 1.08 \text{ cm}^2. \quad (23)$$

It can be verified that the number of contact radii equivalent to the distance between adjacent square contact areas arranged in a square lattice is

$$2(A_a/A_r)^{\frac{1}{2}} \quad (24)$$

regardless of the size of the individual contact area. Therefore, by using expressions (22), (23) and (24), we calculated the repeat distance of the hot spots to be approximately 171 contact radii. The hot spots most likely to interact thermally are those aligned in the direction of tape movement. We measured the length of the wear scar in this direction to be 0.85 cm. By dividing this length by the distance between junctions, we find that the number of these interacting junctions is eight.

In determining surface temperatures near a sliding hot spot on the tape surface, it is sufficient to consider an infinitely long sliding-band source of width $2a$ transversely oriented to the direction of tape movement. Using this model introduces negligible error when temperature distributions in the direction of tape movement are calculated [1]. The solution for the band source is given [1] by

$$\begin{aligned} \frac{T(R)}{T(1)} &= \left(\frac{R+1}{2}\right)^{\frac{1}{2}} && -1 < R \leq 1, \\ &= \left(\frac{R+1}{2}\right)^{\frac{1}{2}} - \left(\frac{R-1}{2}\right)^{\frac{1}{2}} && 1 \leq R \end{aligned} \quad (25)$$

where $R = x/a$, the distance in contact radii behind the center of the moving source, and where $T(R)$ has been

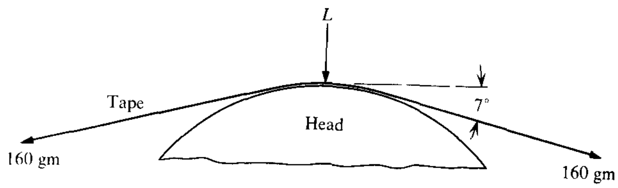

Figure 4 Compression loading at the tape-head interface.

Figure 5 Tape surface temperature profiles for neighboring hot spots.

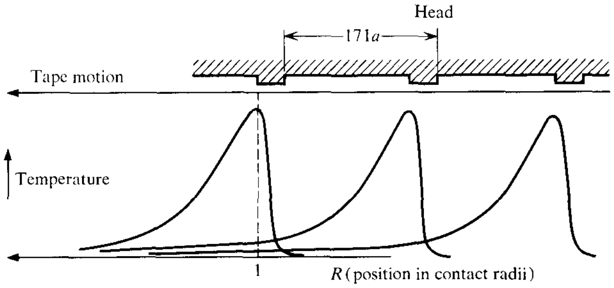

normalized by the maximum temperature which occurs at the trailing edge of the source, i.e., at $R = 1$. When R is large, Eq. (25) can be written

$$\frac{T(R)}{T(1)} = \frac{1}{(2R)^{\frac{1}{2}}} \qquad 1 \ll R. \quad (26)$$

If we assume that there is no thermal interaction among the hot spots, we can use Eq. (25) to plot the profiles of the surface temperature for several adjacent contact areas (see Fig. 5). Notice that should there be any interactions, they would be most strongly felt at the leftmost asperity. Their effect would be to increase the temperature of this asperity over that calculated by Eq. (25).

We can obtain a simple estimate of this interaction by adding the contributions of all eight hot spots at the point $R = 1$ and comparing this to the value for the single hot spot at the point. Using Eq. (25) for the first contact area and Eq. (26) for the remaining seven gives

$$\begin{aligned} \frac{\sum T(R)}{T(1)} &= \left(\frac{R+1}{2}\right)^{\frac{1}{2}} - \left(\frac{R-1}{2}\right)^{\frac{1}{2}} \\ &\quad + \sum_{n=1}^{7} \frac{1}{(2R - 2 + 342n)^{\frac{1}{2}}} \qquad R \geq 1. \end{aligned} \quad (27)$$

When $R = 1$, this gives

$$\frac{\sum T(1)}{T(1)} = 1.22, \quad (28)$$

or a temperature only $\frac{1}{5}$ higher than would have been predicted from a single hot spot. Therefore, the assumption

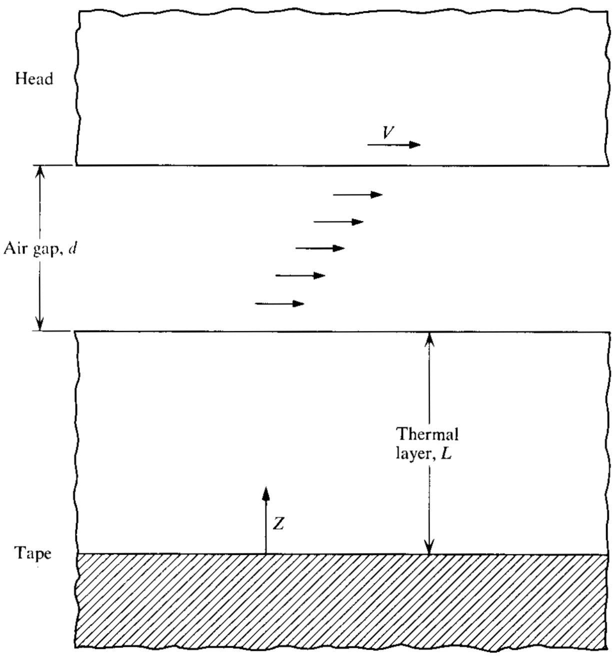

Figure 6 Convective cooling of tape surface.

that there is no thermal interaction among hot spots should not seriously affect the accuracy of the estimate derived from Eq. (4).

To allow for the conservative nature of the three assumptions discussed so far, the estimate given by expression (15) is increased to

$$T \simeq 21^{\circ}\mathrm{C} \tag{29}$$

by the factors given in expressions (18) and (28). The accuracy of this result is directly affected by the approximate nature of the original temperature-rise calculations [see Eqs. (15) and (16)].

Hot spot measurement by infrared microscopy

One popular way to attempt to measure hot spotting at a tape-head interface is to view the tape surface with an infrared radiometric microscope as soon as possible after the tape touches the head. The difficulty with this procedure is that the hot spots usually cool to the ambient tape temperature before the measurement can be taken, thus giving the misleading impression that hot spotting has not occurred. For example, if the surface cools only by conduction into the body of the tape, a 21°C hot spot will cool to 1°C within

$$R = 220 \tag{30}$$

contact radii, or 1.30 mm from the point of contact, according to Eqs. (14) and (26). Few infrared microscopes have a sensitivity of 1°C, and it is difficult to obtain readings as close as 1 mm to the contact zone [10].

Convective cooling of the hot spots to the atmosphere further complicates the problem of temperature measurement. We made the following sequence of approximations to determine how rapidly the hot spots would cool by convection. In each case, the approximation was conservative since a rigorous calculation would have produced an even higher rate of hot spot cooling.

In order to determine the depth of thermal penetration into the tape during the formation of a hot spot, we have written Eq. (19) in the form

$$\frac{T(S,\,t)}{T(0,\,t)} = \frac{\mathrm{ierfc}\,[aS/2(kt)^{\frac{1}{2}}] - \mathrm{ierfc}\,[a(1+S^2)^{\frac{1}{2}}/2(kt)^{\frac{1}{2}}]}{1/\sqrt{\pi} - \mathrm{ierfc}[a\,/2(kt)^{\frac{1}{2}}]} \tag{31}$$

where $S = z/a$, the depth in contact radii below the hot spot, and where $T(S,\,t)$ has been normalized by the hot spot temperature $T(0,\,t)$. The time required to form a hot spot can be approximated by expressions (6) and (14):

$$t = a/V = 2.07 \times 10^{-6}\ \mathrm{sec}. \tag{32}$$

If we consider the depth of thermal penetration to be equal to the level at which a hot spot temperature of 21°C has decayed to 1°C, then by expressions (8), (14), (31) and (32), the thickness of this thermal layer is

$$L = 9.63 \times 10^{-5}\ \mathrm{cm}. \tag{33}$$

We can obtain a conservative estimate of the cooling rate of the tape surface by assuming that the thermal layer cools only by convection into the air gap between the tape and the head. This problem is described in Fig. 6 and by the conditions

$$T(z,\,0) = T_i$$

$$T(z,\infty) = T_f$$

$$\frac{\partial}{\partial z}\,T(0,\,t) = 0$$

$$K\,\frac{\partial}{\partial z}\,T(L,\,t) = h[T_f - T(L,\,t)],$$

for $0 \leq z \leq L$, $0 \leq t \leq \infty$, where

T_i is the initial temperature of the thermal layer
T_f is the ambient air temperature
K is the thermal conductivity of the thermal layer
h is the surface heat-transfer coefficient of the tape.

The solution for the surface temperature of the tape as a function of time [11] is

$$\frac{T(L,\,t) - T_i}{T_f - T_i} = 1 - \sum_{n=1}^{\infty} \frac{2\sin 2\lambda_n}{2\lambda_n + \sin 2\lambda_n}\exp\,(-\lambda_n^{\,2}kt/L^2), \tag{34}$$

where the λ_n's are the roots of the equation [12]

$$\lambda \tan \lambda = hL/K. \tag{35}$$

Before we can use these equations, we must estimate the surface heat transfer coefficient h. The Reynolds number for air flow in the gap between the head and tape surface is quite low, indicating laminar flow [13]. For this condition, heat is transferred through the laminar air layers essentially by conduction. The steady heat flow can be calculated by Fourier's law

$$q = K_a \frac{(T_s - T_h)}{d}, \tag{36}$$

where

T_s is the temperature of the tape surface
T_h is the temperature of the head surface
K_a is the thermal conductivity of air
d is the nominal tape-head gap size.

It is also true that this same rate of heat flow can be expressed [14] as

$$q = h(T_s - T_{AV}), \tag{37}$$

which is the defining relation for coefficient h. The average air temperature, T_{AV}, is $(T_s + T_h)/2$ for laminar flow. Therefore, combining Eqs. (36) and (37) gives

$$h = \frac{2K_a}{d}. \tag{38}$$

The head-to-tape separation for an IBM 2400 series tape drive is

$$d = 7.67 \times 10^{-5} \text{ cm} \tag{39}$$

and the thermal conductivity of air [15] is

$$K_a = 6.37 \times 10^{-5} \text{ cal/(sec)(cm)(°C)}. \tag{40}$$

Therefore,

$$h = 1.67 \text{ cal/(sec)(cm}^2\text{)(°C)}. \tag{41}$$

Equation (34) can now be used with expressions (8), (9), (33) and (41) to estimate the time required to cool a 21°C hot spot to 1°C. This is

$$t = 1.02 \times 10^{-4} \text{ sec}, \tag{42}$$

during which time the tape will have progressed to

$$R = 49.3 \tag{43}$$

contact radii, or 0.291 mm past the point of contact.

The actual rate of convective cooling will be faster than has been estimated here and the hot spots will also cool by inward conduction. Therefore, it does not seem that an infrared microscope can be brought close enough to the tape-head contact zone of an IBM 2400 series tape drive to obtain useful measurements of hot spotting.

Another method of infrared measurement which avoids the problem of rapid cooling of hot spots is to view the contact zone directly through the back side of an infrared-transmitting tape. The limitation here is that when the field of view is larger than the spacing between hot spots, the microscope will read an average surface temperature of the form

$$\frac{T_r A_r + T_a A_a}{A_r + A_a}. \tag{44}$$

The subscripts r and a refer to the real and apparent contact areas, respectively. Unless $T_r A_r$ is of the same order as $T_a A_a$, no increase in the temperature of the tape surface will be detected. For example, according to expressions (22), (23), (29), and for an ambient temperature T_a of 25°C, the average rise in surface temperature for an IBM 2400 series tape drive will be only 0.006°C, which is well below the sensitivity of the infrared microscope.

References and notes

1. J. C. Jaeger, *J. and Proc. Roy. Soc. N.S.W.*, **76**, 203–224 (1942).
2. E. Rabinowicz, *Friction and Wear of Materials*, John Wiley and Sons, Inc., New York, 1965, p. 34.
3. A. J. Ishlinsky, *J. Appl. Math., Mech. (USSR)*, **8**, 233 (1944).
4. E. Rabinowicz, *op. cit.*, p. 89 and Ch. 6.
5. *One-Half Inch Magnetic Tape Specification for Use at 556, 800 BPI, and 3200 fci*, Cat. No. IOSDOI-1, IBM Corp., Information Records Division, Princeton, N. J., December 11, 1967.
6. R. A. Merten, measurement made at IBM Boulder, January, 1968.
7. M. L. Williams, R. F. Landel and J. D. Ferry, *J. Amer. Chem. Soc.*, **77**, 3701 (1955).
8. H. S. Carslaw and J. C. Jaeger, *Conduction of Heat in Solids*, second edition, Oxford University Press, London, 1959, p. 264.
9. F. P. Bowden and D. Tabor, *The Friction and Lubrication of Solids*, Part I, Oxford University Press, London, 1964, Ch. 1.
10. *Instruction Manual for Infrared Radiometric Microscope Model RM-2A*, Barnes Engineering Co., Stamford, Conn., 1966.
11. Carslaw and Jaeger, *op. cit.*, pp. 119, 120.
12. *Ibid.*, Appendix IV.
13. W. L. Badger and J. T. Banchero, *Introduction to Chemical Engineering*, McGraw-Hill Book Co., New York, 1955, pp. 31, 32.
14. *Ibid.*, pp. 125, 126.
15. N. A. Lange, *Handbook of Chemistry*, revised tenth edition, McGraw-Hill Book Co., New York, 1967, p. 1556.

Received October 27, 1969
Revised October 14, 1970

The author is located at the IBM Systems Development Division laboratory at Boulder, Colorado 80301.